Estonian Journal of Earth Sciences, 2015, **64**, 2, 140–158 doi: 10.3176/earth.2015.23

Internal stratification of two thick Ordovician bentonites of Estonia: deciphering primary magmatic, sedimentary, environmental and diagenetic signatures

Sven Siir, Toivo Kallaste, Tarmo Kiipli and Rutt Hints

Institute of Geology at Tallinn University of Technology, Ehitajate tee 5, 19086 Tallinn, Estonia; sven.siir@ttu.ee

Received 2 June 2014, accepted 10 September 2014

Abstract. Twenty-six samples from two major altered volcanic ash beds, Kinnekulle and BII Bentonite of the Kuressaare core section (K-3), Saaremaa Island, were explored to record the geochemical and mineralogical heterogeneity of beds. Signs of ash transport fractionation, redeposition of volcanic ash and diagenetic redistribution of material are described and interpreted. In authigenic mineralogy of the Kinnekulle Bentonite illite–smectite dominates with addition of K-feldspar at the margins. The BII Bentonite is composed of chlorite–smectite and illite–smectite. The stability of phenocryst compositions, including that of sanidine and biotite, indicates that both bentonites originate from a single eruption. The observed rather stable pyroclastic sanidine compositions in the cross section of bentonites confirm the reliability of sanidine-based fingerprinting of altered volcanic ash beds. Trace element distribution in bentonites and host rocks indicates that Zr, Ga, Rb, Nb, Ti and Th stayed largely immobile during volcanic ash alteration and reflect primary ash composition. However, some redistribution of Nb and Ti as well as Y has probably occurred near the contacts of bentonite with the host rock. More scattered grain size distribution and immobile element patterns of the Kinnekulle Bentonite support the idea that the primary ash bed had a heterogeneous composition and it was one of the biggest bentonites of the Phanerozoic and most likely records an extended volcanic event. Significant geochemical variations, including a high S content, near the upper and lower contacts of the Kinnekulle Bentonite and elevated Ca and P in host rocks of both bentonites suggest that the studied large ash-falls caused notable perturbations in shallow marine and early post-sedimentary environment.

Key words: K-bentonite, Mg-bentonite, Ordovician, Estonia.

INTRODUCTION

Volcanic ash fallout is an ‘instantaneous’ event compared to geological time and can be used for precise regional correlation of sedimentary sections (Kolata et al. 1987; Bergström et al. 1995; T. Kiipli et al. 2008a, 2010a, 2010b, 2012, 2014a, 2014b, 2015; Ray et al. 2011; Kaljo et al. 2014; Männik et al. 2014). Volcanic ashes carry also information for the reconstruction of tectonomagmatic environments in volcanic source areas (Batchelor 2009; Hetherington et al. 2011; Kiipli et al. 2013, 2014c). Super-eruptions, ejecting more than 1000 km^3 of dense rock equivalent, transport huge amounts of magmatic material from the Earth’s interior to the surface, some of which freezes immediately as surface rocks, but much of ejected fine material enters the atmosphere as aerosol creating a ‘dark rug’ cover in the upper layers. Aerosols from major blowouts may remain in the atmosphere for up to five years (Rampino et al. 1988) and during this time the influx of solar radiation to the Earth’s surface is impeded, causing global cooling. Lower temperature exerts stress on life and sometimes even causes its extinction after the largest eruptions (Hints et al. 2003; Perrier et al. 2012). Volcanic ash fallouts can also directly affect marine geochemistry, triggering transient acidification of sea water, and quick release of different metals which can either act as nutrients supporting primary production or toxify the marine environment, the latter leading to a possible mass mortality event (e.g. Jones & Gislason 2008; Duggen et al. 2010). Thus, the interaction of primary volcanic ash with different environmental and biotic factors can vary case by case and the signals of these variations may be preserved in the cumulative composition of old volcanic ash beds.

Amorphous glassy material of volcanic ash in sediments alters to clay minerals (commonly smectite) and other authigenic silicates (Grim & Güven 1978), forming bentonites. The primary vertical chemical and mineralogical composition of individual ash beds is not homogeneous (Dahlqvist et al. 2012), but varies due to a successive change in magma composition during long-lasting eruptions and physical fractionation (possibly also chemical alteration) of ash in air transport and settling

in water basins (Fisher & Schmincke 1984). Bergström et al. (1997) and Huff et al. (2010) suggested that in the conditions of an overall slow sedimentation rate and intense volcanism visually homogeneous bentonite layers can accumulate from several volcanic eruptions providing ashes of different compositions. Further, in the course of burial, volcanic ashes are altered by various diagenetic processes (Altaner et al. 1984; Brusewitz 1988; Kiipli et al. 2007; R. Hints et al. 2008).

The aim of this study is to test, describe and interpret the internal heterogeneity of different origins of two major Upper Ordovician bentonite beds in Baltoscandia: the Sandbian Kinnekulle Bentonite of the Keila Regional Stage (Bergström et al. 1995; L. Hints et al. 2008) and the Katian BII Bentonite of the Pirgu Regional Stage (Kiipli et al. 2004, 2015; Hints et al. 2006).

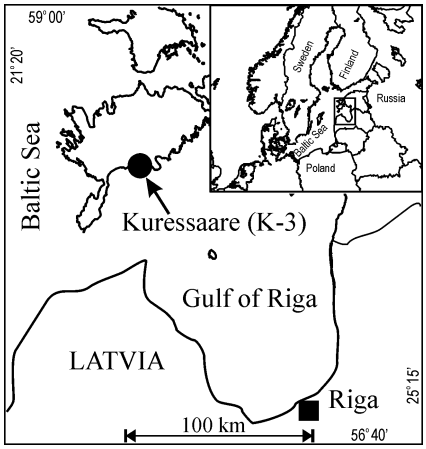

Fig. 1. Location of the Kuressaare (K-3) drill hole in the southern part of Saaremaa Island, Estonia.

MATERIAL AND METHODS

The Kinnekulle Bentonite is the thickest (up to 2 m in the Östergotland area in Sweden and up to 70 cm on Hiiumaa Island in Estonia) and most widely distributed altered volcanic ash bed in the Ordovician of Baltoscandia and the BII Bentonite is the thickest (up to 30 cm) in the Pirgu Stage of Estonia. The ash for both bentonites originated from tectonically active margins of the Iapetus Palaeo-Ocean at a distance of more than 1000–2000 km (Torsvik & Rehnström 2003) from the study site and accordingly both eruptions are considered as very large volcanic events. During their burial and alteration history, the Early Palaeozoic bentonites of the region never reached considerable burial depth and are characterized by low thermal maturity (Somelar et al. 2010).

The material for the current study was collected from the Kuressaare (K-3) drill core from southern Saaremaa Island (Fig. 1), stored at the Keila core depository of the Geological Survey of Estonia. The Kinnekulle Bentonite, marking the boundary of the Haljala and Keila stages, is 40 cm thick and the BII Bentonite in the middle of the Pirgu Stage is 30 cm thick (Figs 2, 3). Host rocks of the Kinnekulle Bentonite are limestones and those of the BII Bentonite, argillaceous marlstones. Based on the facies framework of the Baltic Palaeobasin, the Ordovician sedimentary section of the Kuressaare core belongs to the transition zone between the proximal shallow and deeper shelf sea areas (Põlma 1967).

During sampling both bentonites were divided into eight equal parts, therefore BII samples are 3.75 cm and Kinnekulle samples 5 cm thick. The amount of the study material was about 15–20 g per sample. Host rock samples were taken for comparison at 5 and 30 cm below and at 5 and 15 cm above of the Kinnekulle Bentonite, and at 3, 10 and 20 cm below and above the BII Bentonite layer.

Major chemical components and trace elements were determined by X-ray fluorescence (XRF) methods using a Bruker S4 Pioneer spectrometer. The X-ray tube with the Rh-anode and maximum working power 3 kW was used. Eight grams of fine powder (grains not larger than 50 μm) of samples was mixed with eight drops of 5% Mowiol solution in distilled water and pressed. The pellets were dried for 2 h at 105 °C. The samples were measured and preliminary results were calculated by using the manufacturer's standard methods software MultiRes and GeoQuant. The XRF data in the present study represent the average of these two measurements. Ten international and in-house reference materials were used to refine analytical results by up to a few per cent of the concentration.

Grain material for X-ray diffraction (XRD) and micro-analyses was separated using the following procedure: about 2 g of bentonite samples were dispersed ultrasonically during 2 min in 50 mL of 0.1% Na-pyrophosphate solution. The remaining Na-pyrophosphate suspension was slowly poured away. The pouring must be done very carefully so that the separated grains would not be lost with the suspension of the material. This procedure was performed twice. The next step was adding 25 mL of 1 : 4 HCl solution to the separated grain material for dissolving carbonate minerals and treated with ultrasound until the acid solution became warm and started to steam slightly; the process took about 3 min. According to our experience, this procedure extracts most of the grains larger than 0.04 mm from the bentonite sample.

The XRD measurements of the bulk sample and grain fraction were performed on a D-8 Advance

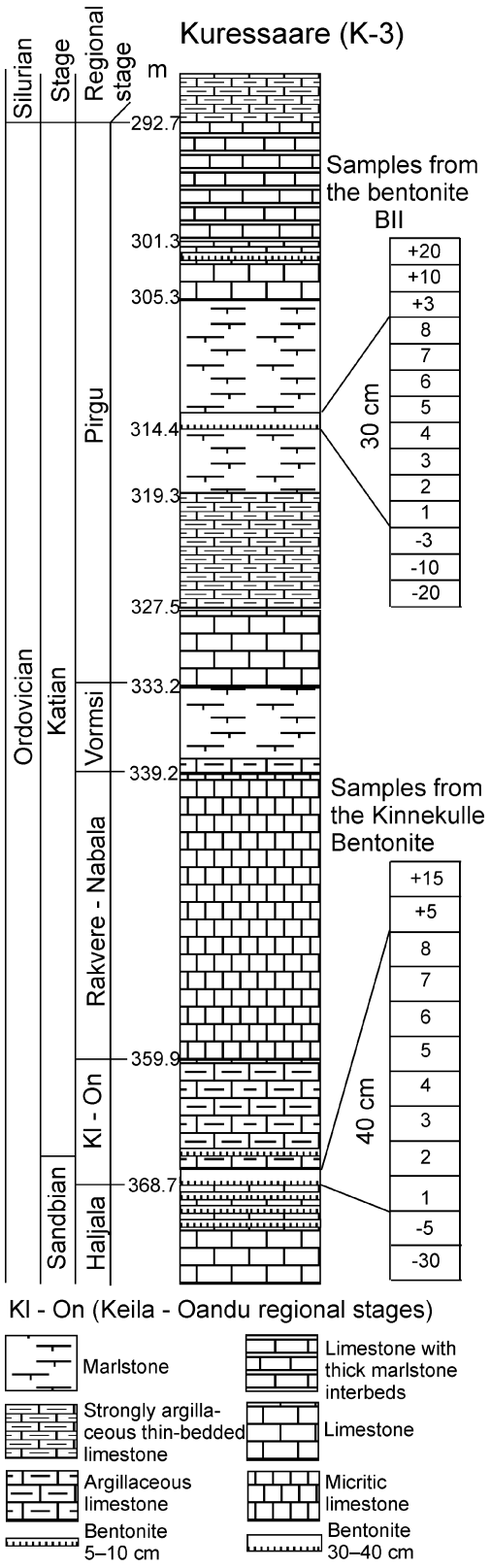

Fig. 2. The lithology and stratigraphy of the Kuressaare (K-3) drill core.

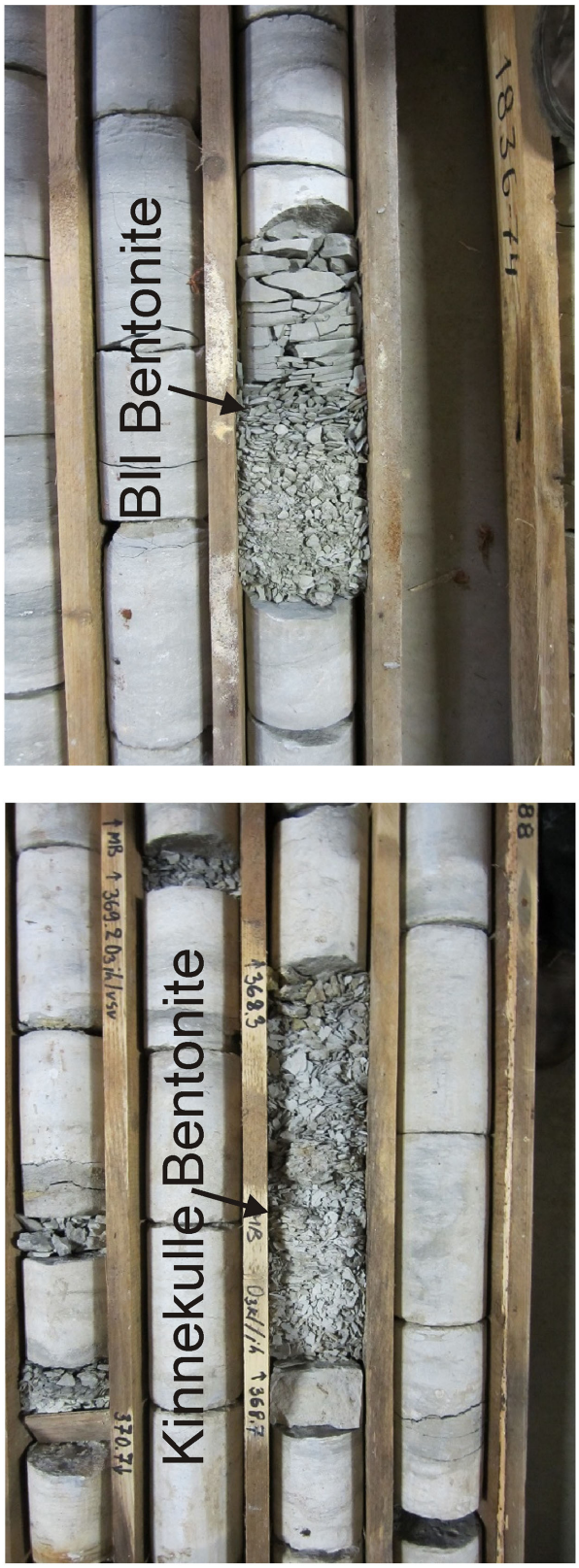

Fig. 3. Drill core photos of the BII and Kinnekulle bentonites.

instrument from Bruker AXS. The measured diffraction patterns were analysed with the TOPAS and EVA software and Microsoft Excel.

Microanalyses of grains were performed with an energy-dispersive X-ray instrument (EDXRF), connected to the scanning electron microscope, under low vacuum (30 Pa) conditions. The electron beam was generated by 20 kV and 650 pA. The basaltic glass BBM-1G, distributed by the International Association of Geoanalysts, was measured together with the studied grains and used as a reference. On the basis of these measurements, Al, Si and Fe concentrations were corrected linearly by a few per cent of the concentration. According to repetitive measurements of BBM-1G, the precision of measurements was better than 0.4%.

RESULTS

XRD analysis of bulk bentonite

Main components of the BII Bentonite detected through the layer are illite–smectite, chlorite–smectite and K-feldspar plus quartz and dolomite (Fig. 4). From these minerals, chlorite–smectite (corrensite) is known only from the bentonites of the Pirgu Stage in Estonia (Hints et al. 2006).

Lower samples of the BII Bentonite are mineralogically quite similar, having a minor amount of calcite and pyrite in sample 1. Small portions of quartz and dolomite appear in sample 3 and these phases consistently increase towards the upper boundary of the bentonite layer. In the upper part of the bentonite (samples 7 and 8) traces of calcite could be observed again. The content of illitic layers in illite–smectite in bentonites of the Pirgu Stage in the East Baltic has been previously reported to vary between 71% and 74% (Hints et al. 2006).

Lower host rock of the BII Bentonite is mostly composed of calcite and dolomite, together with smaller amounts of quartz, illite, K-feldspar, chlorite and traces of pyrite. The host rock just above the bentonite consists mainly of calcite but there are also traces of K-feldspar, quartz and dolomite. The dolomitization and quartz component increase 10 cm above the bentonite, however, this sample is still highly calcitic. This trend continues until 20 cm higher and the rock composition gradually becomes similar to the rock below the bentonite.

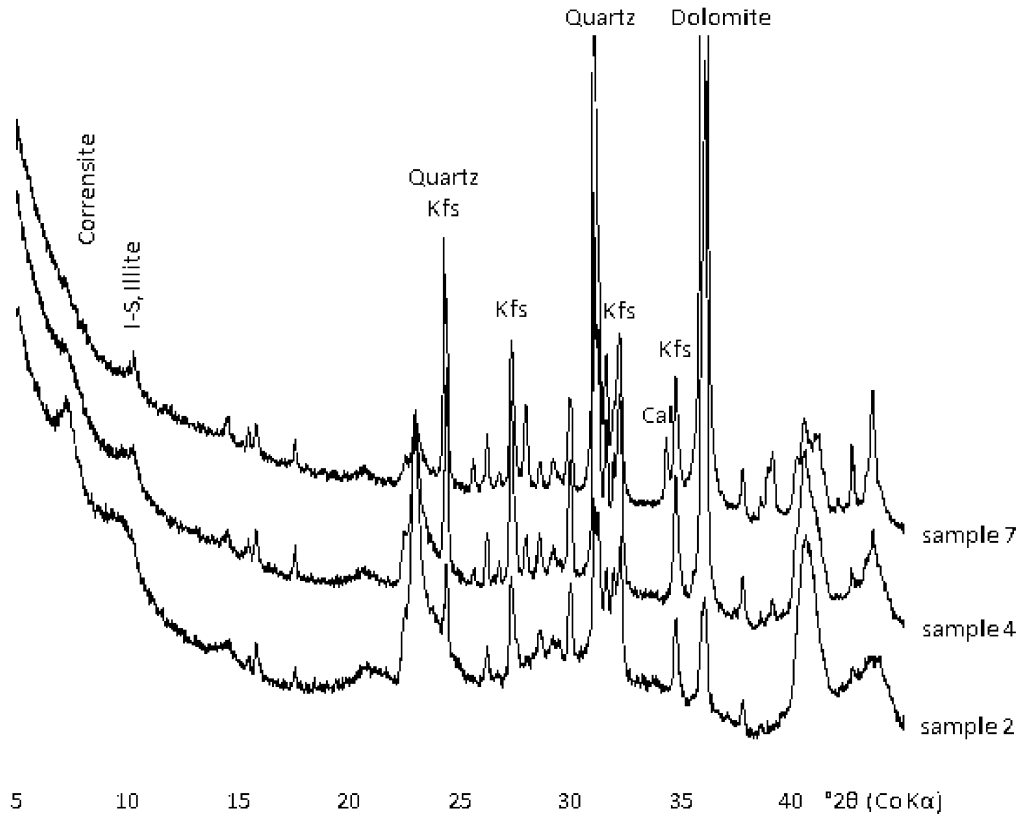

Fig. 4. Examples of XRD patterns from the BII Bentonite. Patterns demonstrate an increase in quartz and dolomite content upwards in the bed. Clay minerals are most abundant in the lower part of the bentonite. I–S, illite–smectite; Kfs, potassium feldspar; Cal, calcite.

Similarly to bentonites, the clay fraction of the host rocks of the Pirgu Stage in the transition zone also contains abundant chlorite–smectite (E. Kiipli et al. 2012).

The mineral composition of the Kinnekulle Bentonite has previously been studied in the Pääsküla exposure, northern Estonia (Hints et al. 1997), where the mineral assemblage of the bentonite was reported to be composed of potassium feldspar and illite–smectite. The same minerals occur in the Kinnekulle Bentonite over the entire northern and central region of Estonia (Kiipli et al. 2007). The content of illitic layers in illite–smectite in the East Baltic area varies between 71% and 87%.

In the Kinnekulle Bentonite of the Kuressaare drill core, illite–smectite occurs as the dominant mineral phase with the highest concentrations in the middle of the bentonite layer. The K-feldspar content is lower than in North Estonian settings, but similarly to those sections the content of K-feldspar reaches the maximum at the upper and lower boundaries of the layer (samples 1, 2 and 8) (Fig. 5).

Major components revealed by XRF analysis

The chemical composition of the two targeted bentonites differs significantly. The most outstanding feature of the compositional variations can be illustrated on the MgO–K_2O chart (Fig. 6). The Kinnekulle Bentonite has a typical K-bentonite composition with the K_2O content around 7% in the middle part. The BII Bentonite has a lower K_2O content (around 5%) and a high content of MgO between 9% and 13%. It suggests that Mg-bentonite could be a more appropriate name for this lithological variety of bentonite. It is distinctive that the host rocks near the BII Bentonite are also enriched in MgO compared with the host rocks of the Kinnekulle Bentonite.

Furthermore, the internal chemical variability patterns of major elements of the BII Bentonite and the Kinnekulle Bentonite possess distinct individual features (Fig. 5). The BII Bentonite shows big differences in geochemistry between the upper and lower parts of the bentonite. SiO_2, Al_2O_3, Fe_2O_3 and MgO follow a similar upward decreasing trend and the differences between the upper and lower parts of bentonite are obvious, whereas the CaO level changes in the opposite direction. Based on the distribution of a number of major components, the Kinnekulle Bentonite is rather uniform throughout the layer. However, it exhibits notably higher K_2O and S contents near both the lower and upper contacts with the host rock. A conspicuous increase in P_2O_5 associated with some rise in CaO occurs in host rocks directly above both bentonites. The host rocks of the bentonites have significantly lower concentrations of all typical elements of silicate minerals and higher contents of CaO than the bentonite beds.

The comparison of the major element composition of bentonites with that of the silicate part of host rocks shows that bentonites contain significantly more Al_2O_3 and less SiO_2 and TiO_2 (Fig. 7). Distinctive is a higher SiO_2 content below the Kinnekulle Bentonite compared with other host rock samples (Fig. 7).

Trace elements revealed by XRF analysis

The studied bentonites have significantly lower concentrations of Ti, Cr and V than the silicate part of host rocks. These elements are therefore good discriminators for recognizing the volcanic origin of clay-rich layers. Higher concentrations of Ti were also recorded in the silicate fraction of host rocks.

The contents of trace elements such as Zr, Th and Nb are higher in the BII Bentonite than in the silicate part of host rocks, but in case of the Kinnekulle Bentonite do not show much difference. Compared to the BII Bentonite, the Kinnekulle Bentonite exhibits notably higher contents of Rb and Ba.

Trace elements vary considerably in the upper and lower parts of the BII Bentonite. Zr reaches 300 ppm in a lower sample and decreases steadily to 100 ppm in the upper part. Ga, Nb, Th, and Rb follow mostly the same pattern and show positive correlation with each other, indicating that these elements stayed largely immobile during the alteration (Fig. 7, Table 1). However, the maximum content of Nb in the silicate fraction of the host rock was recorded directly below the BII Bentonite.

Variations in the trace element content throughout the vertical section of the Kinnekulle Bentonite tend to be smaller but somewhat more irregular than those observed in the BII Bentonite. The most remarkable concentration shifts occur in the uppermost (sample 8) and lowermost (samples 1, 2) parts of the bed. Thus, Ga, Rb and Zr concentrations decrease near the lower and upper contacts (Fig. 7, Table 2). Samples from near the lower and upper contacts of the bentonite bed show also a significant rise in the content of chalcophile elements such as As and Pb, simultaneously with peak S and Fe concentrations. The trace element patterns from the middle part of the bed exhibit small-scale but still notable scattering of immobile trace elements, e.g. of Zr (Table 2, Fig. 8). The higher values of Nb in the silicate fraction of the host rock of the Kinnekulle Bentonite compared to the bentonite values suggest, similarly to the BII Bentonite, mobilization of Nb near the contacts of bentonite with the host rock. The Y values in the bentonite lack good correlation with other typical immobile elements. Its highest concentrations appear in the two

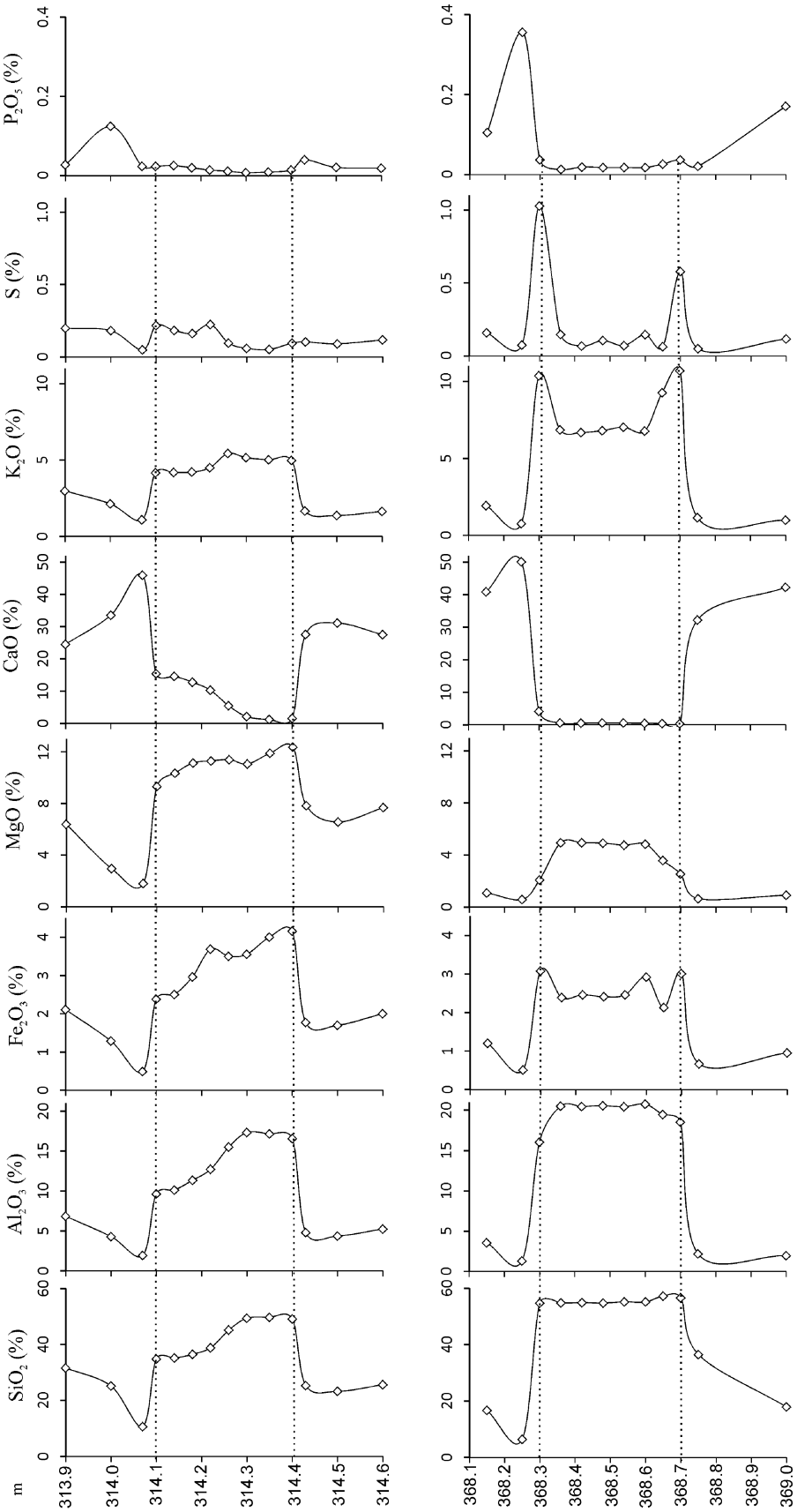

Fig. 5. The distribution of major components in the BII Bentonite (upper panel) and the Kinnekulle Bentonite (lower panel) and host limestones.

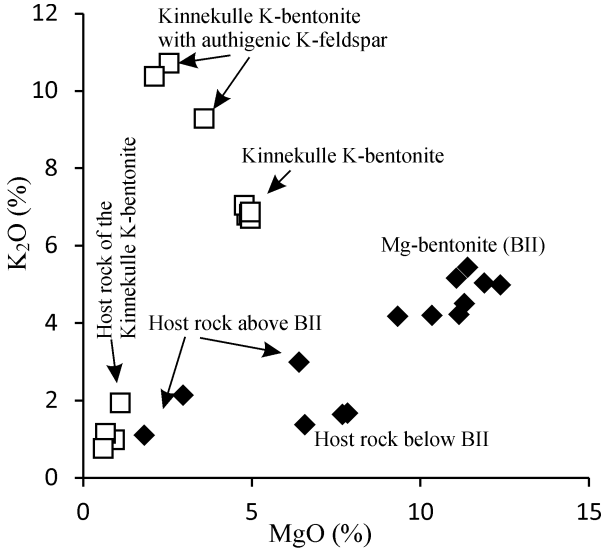

Fig. 6. The composition of two bentonites and host rocks illustrated on the MgO–K_2O chart. The Kinnekulle Bentonite has typical K-bentonite composition but the BII Bentonite shows high contents of MgO.

lowermost samples of the bentonite containing also slightly more P_2O_5 than the rest of samples. Peak concentrations of Y appear directly above the Kinnekulle Bentonite, together with peak values of CaO and P_2O_5.

The composition of grain material and pyroclastic sanidine

Grain material larger than 0.04 mm forms 2–10% of both bentonites. Higher concentrations are found in the lower parts of bentonites with a secondary peak in the third sample from below in the Kinnekulle bed and in the middle of the BII bed. The composition of minerals in grain fraction is presented in Table 3 and pyroclastic material is characterized in Table 4. According to XRD analysis, the authigenic K-feldspar component (end-member orthoclase_313 and K-sanidine, Kastner 1971) forms the major part of grains, varying between 70% and 85% in the Kinnekulle Bentonite. Microanalysis of grains revealed a number of clay aggregates in grain fractions of the BII Bentonite. Conversely, the samples of the Kinnekulle Bentonite were more efficiently purified and did not contain clay. Authigenic pyrite occurs mostly in concentration of 0.5–3.5% in grain fraction, except in the lower and upper samples of the Kinnekulle Bentonite where much higher contents were recorded.

The allogenic (terrigenous + pyroclastic) part (mostly 15–30%) of grains is formed predominantly of K–Na-sanidine (Kastner 1971), quartz and biotite. The quartz component remains at the same level (nearly 6%) within the four lower samples in the BII Bentonite and is followed by an increasing trend upwards. The volcanic sanidine (Na–K-sanidine) component is about 12% within the first six samples (except sample 3 where it reaches 19%), decreasing to nearly 5% in samples 7 and 8. The Kinnekulle Bentonite is rich in biotite (38% of grains measured by microanalysis), while authigenic sanidine forms 48% and Na–K-sanidine only 4% of measurements. Minor phenocrysts are quartz (5%) and apatite (4%).

Among pyroclastic grains the quartz content remains stable, being close to 50% of pyroclasts in the Kinnekulle Bentonite and 24–28% in the BII Bentonite (Table 4). The content of biotite in the Kinnekulle Bentonite decreases upwards and correspondingly the sanidine content rises. The composition of pyroclastic material was not calculated for the upper samples as these contain much terrigenous quartz, indistinguishable from pyroclastic one by XRD. According to XRD, K–Na–Ca-sanidine has a constant composition throughout both bentonite sections, averaging at 25.2 ± 0.6 mol% $(Na,Ca)AlSi_3O_8$ for the Kinnekulle Bentonite and 43.8 ± 0.4 mol% for the BII bed. Measurements of grain compositions by the energy-dispersive XRF (EDXRF) microanalyser confirm the XRD measurements. The composition of biotite detected from the Mg/(Mg + Fe) ratio is also stable throughout the section of the Kinnekulle Bentonite.

The distribution of maximum pyroclastic grain sizes (observed visually under microscope) is homogeneous in the BII Bentonite, staying around 180 μm. On the contrary, the maximum pyroclastic grain size distribution is rather variable in the Kinnekulle Bentonite, being remarkably high (300 μm) in samples 2 and 3, compared to the lowermost and uppermost parts of the bentonite (Table 4, Fig. 9).

DISCUSSION

Multiple- versus single-eruption hypothesis for the source of bentonite-forming material

To explain the origin of some of the major Early Palaeozoic bentonites, a multiple-eruption hypothesis has been put forward (Huff et al. 2010). Nevertheless, the vertical sections of both of the studied bentonites have a stable composition of primary magmatic phenocrysts, as evidenced by the high-precision XRD data of volcanic sanidine (Table 4). Furthermore, sanidine compositional data exhibit good correspondence between XRD and EDXRF data. The Mg/(Mg + Fe) atom ratio in biotite in the Kinnekulle Bentonite was also found to be stable. The observed stability of the composition of primary phenocrysts provides evidence that the magmatic

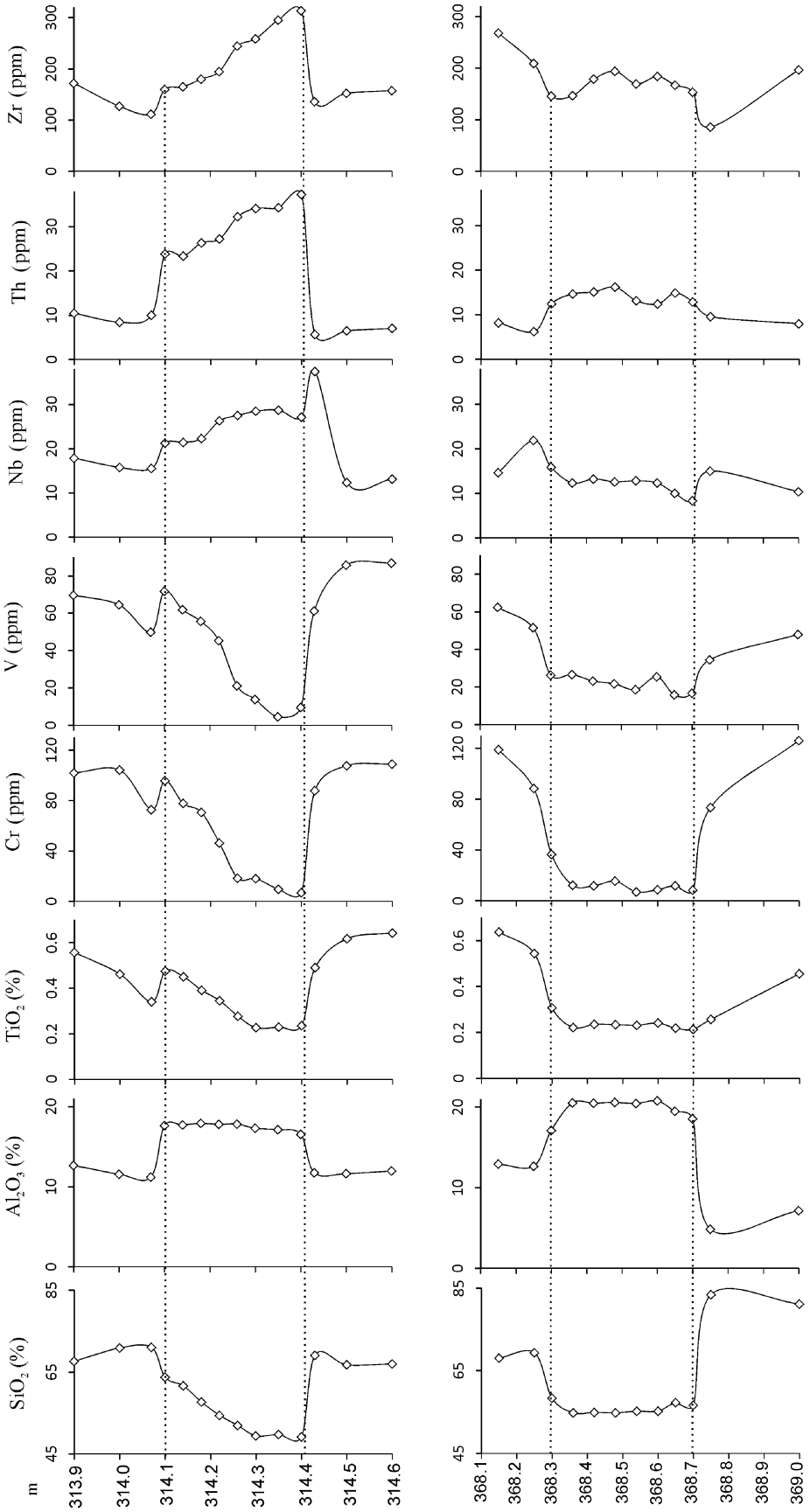

Fig. 7. The distribution of major and trace elements in the silicate fraction of rocks (upper panel – BII Bentonite, lower panel – Kinnekulle Bentonite). The carbonate material from host rock was removed by dissolving in the HCl solution before XRF analyses. For the upper part of the BII Bentonite concentrations were recalculated to the contents within the silicate part of samples.

Table 1. Major and trace element contents in the BII Bentonite and host rock

	Sample/depth (m)/lithology													
	BII –20/ 314.60/ limestone	BII –10/ 314.50/ limestone	BII –3/ 314.43/ limestone	BII_1/ 314.40/ bentonite	BII_2/ 314.35/ bentonite	BII_3/ 314.30/ bentonite	BII_4/ 314.26/ bentonite	BII_5/ 314.22/ bentonite	BII_6/ 314.18/ bentonite	BII_7/ 314.14/ bentonite	BII_8/ 314.10/ bentonite	BII +3/ 314.07/ limestone	BII +10/ 314.00/ limestone	BII +20/ 313.90/ limestone
Major elements (%)														
LOI 920°	31.0	32.3	31.4	9.1	8.9	10.1	13.6	19.2	22.2	24.1	24.4	37.1	29.6	25.6
SiO_2	25.7	23.3	25.4	49.2	49.8	49.4	45.2	38.9	36.5	35.2	34.8	10.7	25.2	31.7
TiO_2	0.216	0.185	0.191	0.236	0.230	0.227	0.241	0.247	0.248	0.258	0.260	0.051	0.154	0.240
Al_2O_3	5.3	4.4	4.8	16.6	17.2	17.3	15.5	12.7	11.4	10.1	9.7	2.0	4.3	6.9
Fe_2O_3	2.0	1.7	1.8	4.2	4.0	3.6	3.5	3.7	3.0	2.5	2.4	0.5	1.3	2.1
MnO	0.053	0.047	0.054	0.007	0.006	0.008	0.018	0.032	0.038	0.040	0.039	0.028	0.039	0.043
MgO	7.7	6.6	7.8	12.4	11.9	11.1	11.4	11.3	11.1	10.4	9.3	1.8	3.0	6.4
CaO	27.5	31.1	27.6	1.6	1.3	2.2	5.5	10.3	12.9	14.6	15.5	45.9	33.6	24.6
Na_2O	0.07	0.06	0.06	0.24	0.24	0.27	0.25	0.25	0.20	0.16	0.15	0.03	0.08	0.11
K_2O	1.6	1.4	1.7	5.0	5.0	5.2	5.4	4.5	4.2	4.2	4.2	1.1	2.1	3.0
P_2O_5	0.019	0.021	0.040	0.014	0.010	0.008	0.011	0.014	0.020	0.026	0.024	0.024	0.124	0.028
Cl	0.022	0.021	0.021	0.010	0.009	0.008	0.010	0.013	0.016	0.018	0.024	0.023	0.028	0.023
S	0.12	0.09	0.10	0.10	0.05	0.06	0.10	0.23	0.16	0.18	0.22	0.05	0.18	0.20
F	0.12	0.10	0.10	0.54	0.54	0.56	0.44	0.51	0.42	0.28	0.27	0.03	0.05	0.17
Trace elements (ppm)														
As	2	2	1	4	3	3	3	6	5	4	4	0	0	3
Ba	138	121	117	29	50	61	78	83	53	69	116	20	94	137
Cr	44	35	37	7	10	18	16	33	45	45	52	16	40	53
Cu	8	11	7	5	3	4	2	7	6	6	6	8	5	7
Ga	5	3	5	17	18	18	15	12	10	10	8	<5	3	6
La	17	19	26	8	8	16	19	15	12	1	11	37	<20	14
Nb	5	4	9	27	29	28	24	19	14	12	12	4	7	7
Ni	16	14	17	34	34	30	35	41	31	25	22	6	13	23
Pb	6	11	13	8	9	7	9	14	10	9	12	9	13	8
Rb	48	42	43	97	100	100	87	69	64	64	64	14	36	52
Sc	<20	<20	<20	0	<20	19	18	<20	<20	<20	13	<20	9	<20
Sn	<10	<10	<10	7	6	7	5	5	4	3	2	<10	<10	<10
Sr	221	275	192	72	77	77	70	74	79	86	96	474	361	290
Th	5	4	6	37	34	34	28	19	17	13	13	0	6	9
U	<5	0	2	6	7	4	5	5	3	3	4	<5	<5	<5
V	39	35	33	10	5	14	18	32	35	35	39	18	23	34
Y	15	13	14	29	26	20	17	12	13	14	14	10	17	17
Zn	19	17	18	18	16	18	20	25	24	24	22	6	15	22
Zr	51	46	49	314	296	259	213	139	114	94	87	26	45	73

Table 2. Major and trace element contents in the Kinnekulle Bentonite and host rock

	Sample/depth (m)/lithology											
	Kin –30/ 369.00/ limestone	Kin –5/ 368.75/ limestone	Kin 1/ 368.70/ bentonite	Kin 2/ 368.65/ bentonite	Kin 3/ 368.60/ bentonite	Kin 4/ 368.54/ bentonite	Kin 5/ 368.48/ bentonite	Kin 6/ 368.42/ bentonite	Kin 7/ 368.36/ bentonite	Kin 8/ 368.30/ bentonite	Kin +5/ 368.25/ limestone	Kin +15/ 368.15/ limestone
Major elements (%)												
LOI 920°	32.9	24.3	5.0	5.3	7.1	6.9	7.4	7.3	7.5	6.1	38.6	31.9
SiO_2	18.0	36.6	56.7	57.3	55.3	55.2	54.9	55.0	54.9	54.8	6.5	16.8
TiO_2	0.122	0.124	0.214	0.219	0.241	0.231	0.234	0.236	0.222	0.289	0.053	0.183
Al_2O_3	2.0	2.2	18.6	19.5	20.8	20.5	20.6	20.5	20.5	16.1	1.3	3.6
Fe_2O_3	1.0	0.7	3.0	2.1	2.9	2.5	2.4	2.5	2.4	3.1	0.5	1.2
MnO	0.040	0.036	0.008	0.008	0.008	0.009	0.008	0.009	0.007	0.009	0.046	0.042
MgO	0.9	0.7	2.5	3.6	4.8	4.8	4.9	5.0	5.0	2.1	0.6	1.1
CaO	42.3	32.2	0.4	0.4	0.5	0.6	0.6	0.6	0.6	4.2	50.2	40.9
Na_2O	0.04	0.04	0.18	0.26	0.37	0.37	0.37	0.39	0.43	0.21	0.04	0.09
K_2O	1.0	1.2	10.7	9.3	6.8	7.0	6.8	6.7	6.9	10.4	0.8	1.9
P_2O_5	0.171	0.021	0.037	0.027	0.018	0.018	0.018	0.019	0.013	0.037	0.356	0.105
Cl	0.031	0.028	0.016	0.022	0.029	0.032	0.032	0.031	0.042	0.036	0.031	0.038
S	0.12	0.05	0.58	0.06	0.15	0.07	0.11	0.07	0.15	1.03	0.08	0.16
F	0.02	0.03	0.20	0.34	0.40	0.39	0.38	0.41	0.42	0.15	0.04	0.02
Trace elements (ppm)												
As	4	1	13	3	4	3	3	1	6	35	2	1
Ba	33	30	195	156	175	158	147	185	129	116	5	51
Cr	34	43	9	12	9	7	16	12	12	34	14	38
Cu	10	5	5	3	3	4	3	1	2	10	7	7
Ga	1	2	12	17	22	23	22	23	22	13	<5	3
La	26	20	8	8	6	8	<20	<20	10	9	36	24
Nb	4	8	8	10	12	13	13	13	12	15	3	6
Ni	9	7	12	17	16	9	7	7	6	20	2	7
Pb	5	9	10	6	8	7	7	8	9	26	13	11
Rb	25	27	98	113	130	126	127	128	122	85	16	37
Sc	<20	14	5	17	10	28	9	0	<20	2	2	<20
Sn	<10	<10	8	8	10	8	7	10	8	7	<20	<10
Sr	191	141	38	58	78	79	77	79	80	74	198	264
Th	4	4	13	15	12	13	16	15	15	12	7	8
U	<5	3	4	3	3	4	6	3	2	4	5	3
V	17	25	17	16	25	19	22	23	27	25	8	24
Y	21	13	22	24	20	21	18	20	14	16	49	23
Zn	6	7	10	10	12	12	11	12	11	11	5	11
Zr	49	42	154	167	184	170	194	179	147	137	21	77

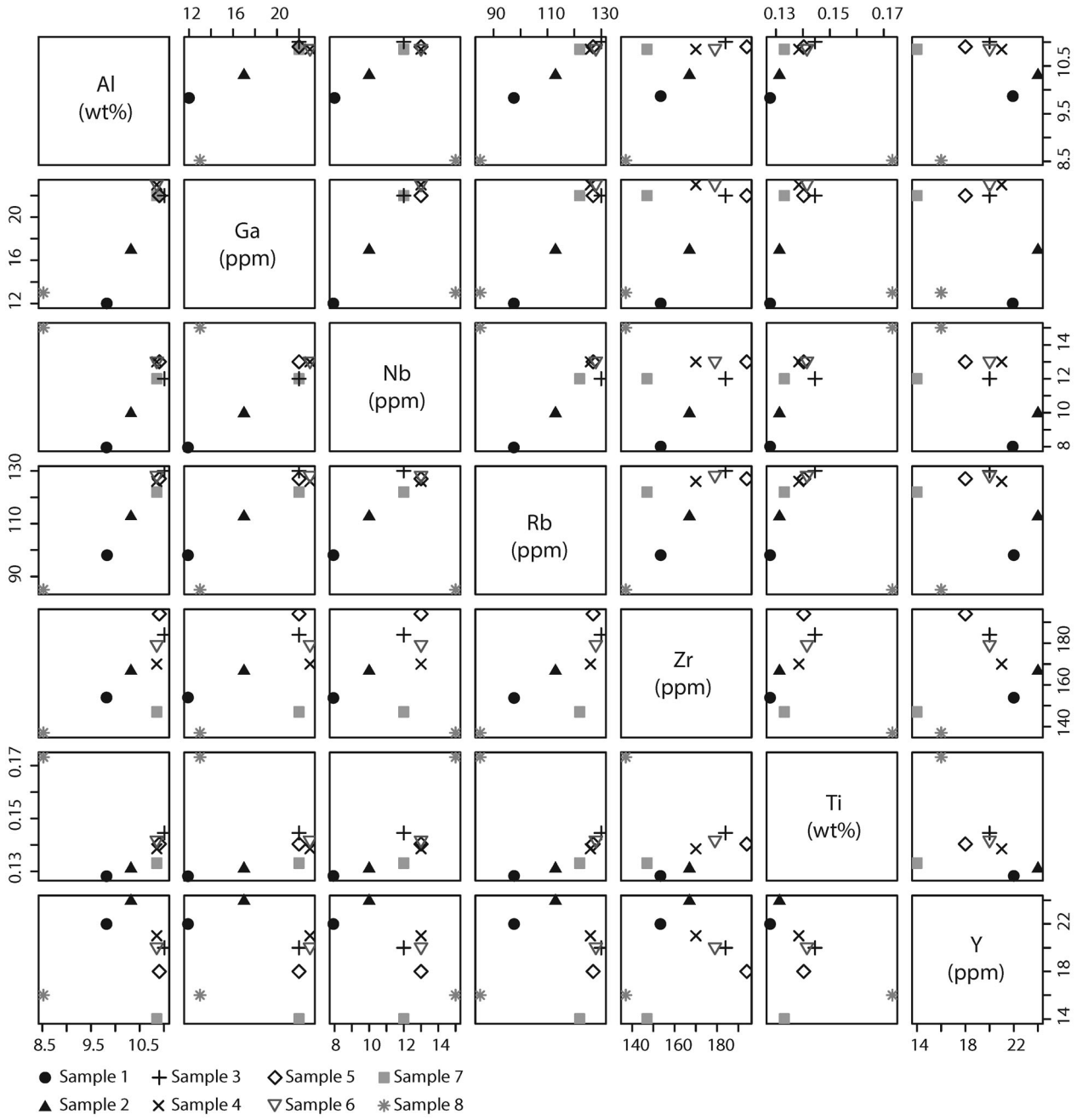

Fig. 8. Scatterplot matrix showing immobile element distribution in the cross section of the Kinnekulle Bentonite. The graphic presents pairwise relations of Al, Ti, Ga, Nb, Rb, Zr and Y. In case of homogeneous source material the ratios of immobile elements are expected to remain constant during ash alteration. However, for the Kinnekulle Bentonite the trace element scatterplots reveal notable variations between different samples, which might suggest either primary geochemical inhomogeneity of source material or diagenetic redistribution. Samples close to the upper and lower contacts of the bentonite (samples 1, 2 and 8) are characterized by a somewhat different immobile trace metal behaviour than the samples from the middle part of the bentonite. Those samples also have the lowest Al content. Samples 3–6 are characterized by a considerably homogeneous trace element composition. The distribution of Zr in the middle part of the Kinnekulle Bentonite, however, does not show good correlation with that of Al and with other immobile trace elements. Y demonstrates a rather different behaviour with respect to other immobile elements in the upper and lower parts of the bentonite.

Table 3. The composition of major minerals in the grain fraction

	Kinnekulle Bentonite						BII Bentonite							
	Biotite		Magmatic sanidine		Authigenic sanidine		Authigenic sanidine		Magmatic sanidine		Authigenic aggregates			
											Mostly illite–smectite		Mostly chlorite–smectite	
	n = 51		*n* = 5		*n* = 53		*n* = 47		*n* = 16		*n* = 7		*n* = 7	
	%	STD	%	STD	%	STD	%	STD	%	STD	%	STD	%	STD
Na_2O	0.37	0.07	2.51	0.09	0.06	0.04	0.10	0.05	4.35	0.22	0.10	0.06	0.04	0.02
MgO	6.97	0.46	0.06	0.03	0.11	0.15	0.29	0.14	0.24	0.17	7.99	0.65	14.96	0.77
Al_2O_3	16.44	0.36	18.36	0.09	17.82	0.18	17.67	0.21	18.61	0.39	17.53	1.13	15.09	0.93
SiO_2	39.06	1.16	62.83	0.51	62.55	0.59	63.07	0.48	63.83	1.03	60.56	0.62	57.13	0.96
S	0.15	0.19	0.12	0.09	0.08	0.08	0.10	0.13	0.09	0.07	0.21	0.09	0.38	0.26
K_2O	9.23	0.25	11.72	0.08	15.59	0.26	15.41	0.23	9.01	0.30	6.70	0.49	3.52	0.17
CaO	0.16	0.09	0.32	0.06	0.15	0.11	0.09	0.05	0.47	0.22	0.57	0.06	0.63	0.11
TiO_2	4.44	0.33	0.11	0.10	0.09	0.10	0.02	0.06	0.01	0.04	0.31	0.25	0.10	0.10
MnO	0.23	0.04	0.05	0.02	0.01	0.03	0.00	0.03	0.00	0.04	0.01	0.04	0.02	0.03
FeO	22.49	1.35	0.55	0.21	0.63	0.50	0.27	0.17	0.32	0.12	2.84	0.86	4.57	0.38
BaO	0.38	0.11	0.40	0.17	0.06	0.08	0.02	0.07	0.27	0.56	0.04	0.05	0.02	0.07
Index in the chemical formula														
Na	0.06	0.01	0.24	0.01	0.01	0.00	0.01	0.00	0.41	0.02				
K	0.94	0.01	0.74	0.01	0.99	0.01	0.99	0.01	0.56	0.02				
Ca	0.02	0.01	0.02	0.00	0.01	0.01	0.01	0.00	0.02	0.01				
Ba	0.01	0.00	0.01	0.00	0.00	0.00	0.00	0.00	0.01	0.01				
Mg	0.95	0.06	nc	nc	nc	nc	nc	nc	nc	nc				
Fe	1.70	0.06	0.02	0.01	0.02	0.02	0.01	0.00	0.01	0.00				
Ti	0.30	0.02	nc	nc	nc	nc	nc	nc	nc	nc				
Mn	0.02	0.00	nc	nc	nc	nc	nc	nc	nc	nc				
Al	1.32	0.03	1.02	0.01	1.00	0.01	0.99	0.01	1.02	0.03				
Si	2.67	0.03	2.96	0.02	2.98	0.02	3.00	0.01	2.97	0.03				
Biotite:	(K,Na)1(Mg,Fe,Ti,Ca)3(Al,Si)4O10(OH,F)2						Feldspars:		(K,Na,Ca,Ba)1(Si,Al,Fe)4O8					

n, number of measurements; nc, not calculated.

Table 4. Characterization of the pyroclastic material

Depth (m)	XRD results				EDXRF microanalyses results			Micoscope
	Quartz in pyroclasts (%)	Biotite in pyroclasts (%)	Sanidine in pyroclasts (%)	Na + Ca in sanidine (mol%)	Na + Ca in sanidine (mol%)	Mg/(Mg + Fe) atom ratio in biotite	Other minerals	Maximum size of pyroclastic grains (μm)
BII Bentonite								
314.10	nd	0.0	nd	44.0	nd			nd
314.14	nd	0.0	nd	44.0	43.8		Quartz	170
314.18	nd	0.0	nd	43.6	nd			180
314.22	nd	0.0	nd	44.1	43.1		Quartz	180
314.26	nd	0.0	nd	44.0	nd			170
314.30	23.9	0.0	76.1	43.7	43.2		Quartz	180
314.35	27.0	0.0	73.0	43.5	43.3		Quartz	180
314.40	27.7	0.0	72.3	43.5	43.9		Quartz, TiO_2	190
Kinnekulle Bentonite								
368.30	nd	nd	nd	nd	nd	nd		180
368.36	49.4	6.1	44.6	25.2	26.4	0.36	Quartz	200
368.42	52.2	7.9	39.9	25.3	nd	nd		210
368.48	52.7	7.0	40.3	25.0	nd	0.35	Quartz	200
368.54	52.0	12.4	35.6	25.1	nd	nd		220
368.60	55.1	16.9	27.9	24.9	25.7	0.35	Quartz, apatite	300
368.65	52.9	16.2	30.9	25.2	24.7	0.37	Quartz, apatite	300
368.70	48.2	21.4	30.5	26.0	25.6	0.37	Quartz, apatite	230

nd, not determined.

material most likely originated from a single volcanic eruption for both bentonites.

On the other hand, notable grain size difference of pyroclastic minerals was documented across the section of the Kinnekulle Bentonite. As a rule, coarser grain material falls first from volcanic ash clouds and consequently the lower part of the bentonite must contain larger grains than the upper part. However, while the grain size in the BII Bentonite perfectly follows this rule, in the Kinnekulle Bentonite the maximum primary grain size was found in the second and third samples from below. This may indicate relatively long duration of the Kinnekulle eruption. The deposition of larger grains in the middle of an eruption can be caused by a temporary rise in the power of the eruption or change in wind direction. The pyroclastic grain distribution of the BII Bentonite shows no obvious signatures of primary volcanogenic or air-transport-induced heterogeneity and this bentonite probably originates from a shorter eruption. The recorded immobile trace element distribution patterns in the studied sections do not contradict the concept of the single-eruption origin of both bentonites. However, variations in the contents of some minor elements (e.g. Zr, Rb, P_2O_5) in the Kinnekulle bed could reflect notable variations in pyroclastic minerals input during sedimentation.

Role of the mixing of material during transport and emplacement

The Zr content in the BII Bentonite is the highest in the lower sample and decreases upwards. As this trend occurs already in lower samples, it cannot be explained by redeposition and points to the fractionation of material already during air transport. Obviously the phenocrysts larger and heavier (e.g. zircon) than vitric particles deposited faster and accumulated in the lower part of the ash bed. In case of the Kinnekulle Bentonite the heterogeneity of the primary ash layer is signalled by somewhat irregular distribution of Zr content across the section, with the highest concentrations in sample 5.

Ash deposition in shallow-water marine environments might be accompanied by considerable redeposition and mixing of primary ash with regular marine sediments. Terrigenous and calcareous admixture in the Kinnekulle Bentonite is noticeable only in the upper sample, as indicated by slightly elevated values of CaO and Cr. Data for the BII Bentonite, however, suggest that the upper part of the bentonite layer was mixed with marine calcareous mud and terrigenous material (Fig. 7). Judging from the absence of carbonate material and low content of Ti, Cr and V, the 3–4 lower samples represent pure bentonite. The admixture of terrigenous and carbonate

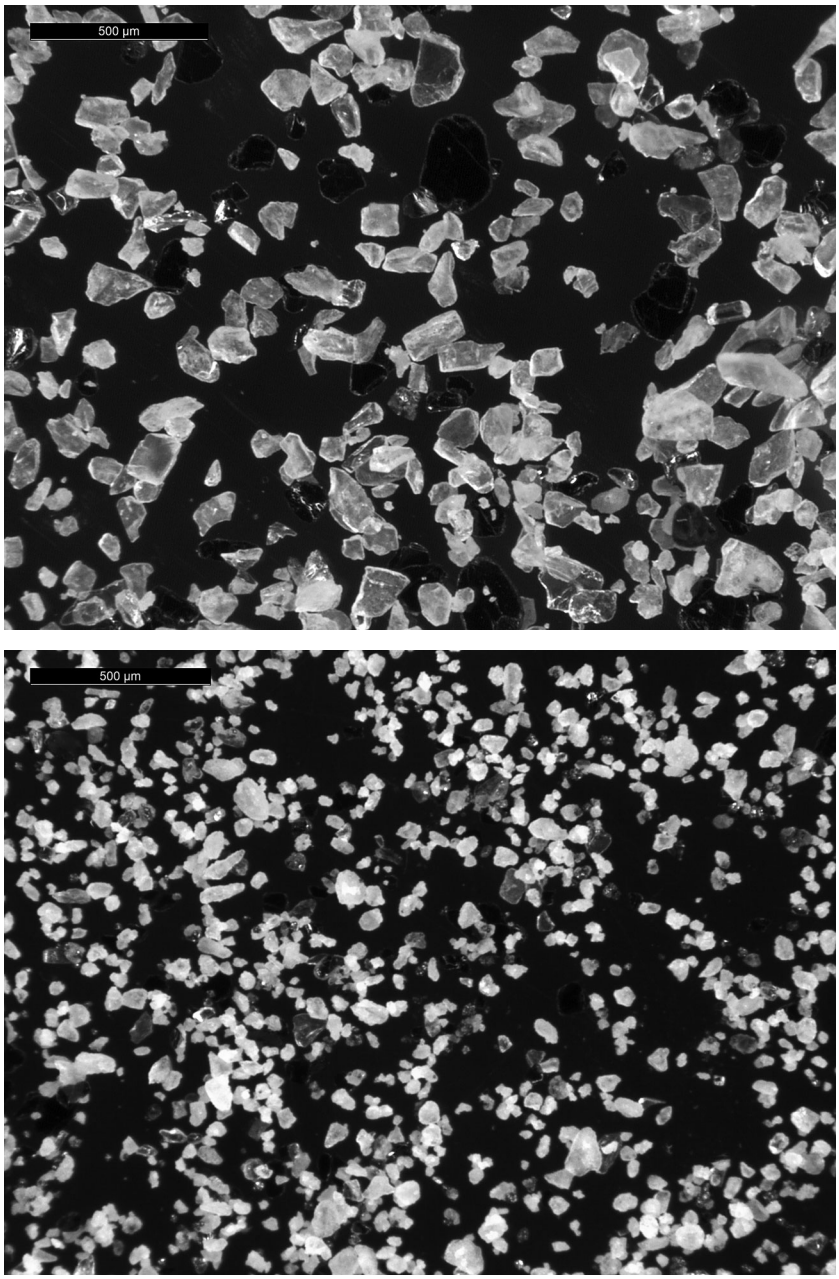

Fig. 9. Photographs of the grain fraction of the Kinnekulle Bentonite showing much larger grains in sample 3 (upper image) than in the lowermost sample 1 (lower image).

sedimentary material increases upwards starting from sample 4, as seen from the content of dolomite in bulk samples (Fig. 4) and an increase in Ti, Cr and V. Thus, geochemical trends indicate that the full section of the primary ash layer of the BII Bentonite formed under a combination of two physical processes: (1) direct fall-out of ash from the atmosphere and (2) reworking and redeposition of ash during transport from shallow- to deeper-marine environments.

Diagenetic alteration

While SiO_2 contents are high in evolved source magmas (e.g. between 60% and 80%), the concentrations in bentonites are typically significantly lower (e.g. between 40% and 60%), indicating the dissolution and removal of silica during the transformation of volcanic ash to authigenic minerals. The source magma composition of the Kinnekulle Bentonite has been determined from

glass inclusions in quartz phenocrysts (Huff et al. 1996). These analyses showed approximately 78% SiO_2 and 13% Al_2O_3. After diagenetic alteration the SiO_2 contents of bentonite are much lower – around 55%. The removal of SiO_2 from ash beds could be indicated by the accumulation of authigenic chert below thick ash beds (Grim & Güven 1978) and less frequently above them. In our case unusually high SiO_2 contents reaching 80% (Fig. 7) in the silicate part of host rock below the Kinnekulle Bentonite most likely indicate silica leaching from the bentonite. The process is similar to the silicification of conodonts (Laufeld & Jeppson 1976). The absence of elevated SiO_2 contents above the BII Bentonite suggests that either (1) early release of silica was mostly completed before the deposition of layers above, or that (2) the system was open enough to support effective migration of dissolved silica. Among other major components Na_2O, common in source magmas, has been almost completely dissolved and removed. Only small amounts of Na_2O are preserved within sanidine phenocrysts in both bentonites.

The rest of less soluble residual material has altered into clay minerals and authigenic potassium feldspar. During authigenic mineral formation, ash assimilated some elements from the surrounding environment, whereas the set of assimilated elements has been considerably different in the Kinnekulle and BII bentonites. The most obvious difference is the incorporation of Mg during the alteration of primary ash of the BII Bentonite. The content of Mg is low in the evolved source magmas (for example 0.07% in the source magma of the Kinnekulle ash, Huff et al. 1996), i.e. the observed 11–12% of MgO in the BII Bentonite and 5% in the Kinnekulle Bentonite should be predominantly of authigenic origin. Hints et al. (2006) explained the formation of high-Mg chlorite–smectite-rich bentonites under the influence of saline evaporitic waters from sabkhas of the Pirgu Age. Although hypersaline sediments of the Pirgu Age are not known in Estonia, sedimentary diagenetic dolomites occur in younger Hirnantian sediments. So it is possible that initially lagoonal environments existed also in the Pirgu Age and these primary sediments have been eroded later. The outflow of lagoonal waters along the seafloor to the open sea of the transition zone may explain both: partial dolomitization of host rocks of Pirgu age and the occurrence of chlorite–smectite in host rocks (Kiipli et al. 2012). Higher temperature in Pirgu time, possibly favouring the development of evaporitic settings, is supported by Fortey & Cocks (2005). On the basis on the movement of tropical fauna to lower latitudes, they showed a global warming in Katian time. In contrast, the limestones around the Kinnekulle Bentonite are considered to have been deposited in cold water conditions as the Baltica plate was located at that time in intermediate latitudes in the southern hemisphere (Torsvik & Rehnström 2003). Being deposited under normal marine conditions, the ash of the Kinnekulle Bentonite converted mostly to illite–smectite during alteration, the illitization process controlled by external K-flux.

Similarly to illite–smectite, the formation of authigenic K-feldspar in bentonites needs an external source of K. High potassium contents reaching 10% at the margins of the Kinnekulle Bentonite cannot be supplied from volcanic ash where the initial K_2O content was 4% (Huff et al. 1996). The K_2O content can exceed 15% in other sections (Kiipli et al. 2007). A number of hypotheses have been put forward to explain the formation of K-feldspar and incorporation of additional potassium into bentonites. Kiipli et al. (2007) suggested that high pH in shallow-sea environments enables incorporation of cations from sea water, favouring the formation of feldspars instead of H^+ in low-pH conditions, which leads to the formation of clay minerals. R. Hints et al. (2008) suggested that authigenic feldspar in Estonian bentonites might be a product of recrystallization of early diagenetic metastable zeolites, formed due to the interaction of ash and juxtaposed highly alkaline calcareous muds. Somelar et al. (2010) concluded that significant influx of potassium controlling illitization of smectite in Early Silurian bentonites was caused by regional saline fluids flowing into sedimentary rocks significantly later than the deposition time.

Late diagenetic formation of K-feldspar (or its precursor phase) in bentonites is, however, problematic because of frequent alternation of bentonites of different composition in sections. For example, the Kuressaare drill core contains the following bentonites: 368.7 m – illite–smectite with K-feldspar addition at margins, 314.4 m – chlorite–smectite with illite–smectite (present study), 215.7 m – 7 cm of pure K-feldspar, 214–158 m – 16 thin bentonite layers consisting of illite–smectite including a K-feldspar layer at 184.8 m (Kallaste & Kiipli 2006; Kiipli et al. 2006). According to R. Hints et al. (2008), the upper part of the Kinnekulle Bentonite in the Põõsaspea exposure (Northwest Estonia), includes a layer of sedimentary breccia where angular grains consist of pure K-feldspar, while the fine-grained mass of breccia contains terrigenous clay and carbonates. This indicates that the hardened layer in the upper part of the bentonite had already formed before a storm event brecciated it, strongly supporting an early start of the recrystallization of primary ash.

Supposing that Al_2O_3 was immobile (13% in source magma and 20% in bentonite) during the conversion of

volcanic ash to clay and feldspar, we see that concentrations of immobile elements in the Kinnekulle Bentonite have risen 1.5 times compared with source magma. In our previous analyses on the East Baltic materials we have considered Ti, Zr, Th and Nb as immobile (Kiipli et al. 2008b, 2013). The present data from the BII Bentonite, where the maximum Nb content significantly exceeding common values in the silicate parts of the host rock occurs directly below the bentonite, indicate small-scale mobility of this element during the conversion of volcanic ash in lime sediment. Although small-scale mobility to a distance of a few centimetres may not exclude the use of Nb in the interpretation of source magma, still, care should be taken when using this element in particular cases. In the samples of the Kinnekulle Bentonite, for example, the Nb/Y ratio, commonly used for discriminating magma series (Winchester & Floyd 1977), was found to vary from 0.4 to 0.9. However, this considerably large variation is largely dependent on the irregular distribution of Y, whose content in beds was likely controlled by combined factors such as the input of pyroclastic apatite and leaching of elements near the upper contact of the ash bed.

Environmental effects of ash-falls and interaction of the ash–water–sediment system

Some previous works have reported a marked decrease in the diversity of marine life after the deposition of the thick Kinnekulle Bentonite (Hints et al. 2003; Perrier et al. 2012) and interpreted those variations as consequences of environmental perturbations caused by volcanic eruptions. The geochemical signatures recorded in bentonites and their host rocks by the current study demonstrate that both studied large ash-falls, but more notably the Kinnekulle ash-fall, triggered environmental changes in marine settings where they were deposited. The direct effect of the ash-fall can be read from the peaks of sulphur below and above the Kinnekulle Bentonite. Sulphur fixation in sediments occurs when organic material is decayed in an anoxic environment via microbial sulphate reduction. Life forms on the sea bottom possibly died at the lower contact of the primary ash layer as a result of abrupt burial under the ash, which initially could be up to 1 m thick, and thus promoted the development of anoxia below. Water-soluble ash leachates could additionally provide an extra source of sulphate for sulphate reduction near a freshly deposited ash layer. It is also possible that ash-fall was accompanied by toxification of the water column and mass mortality. The deposition of dead organic matter on the sea floor could have been slower than of volcanic dust due to its better flotation properties. Consequently the organic matter could accumulate in the upper layers of the ash bed, thus explaining sulphur accumulation in the upper layer of bentonite. Alternatively, an ash-fall could trigger an increase in primary production through fertilizing the water column with essential macro- and micronutrients (e.g. Duggen et al. 2010). The resultant rise in organic matter flux to the shallow sea bottom could promote quick consumption of free oxygen and sulphate reduction.

The absence of sulphur peaks at the margins of the BII Bentonite may be caused by a shorter duration of the eruption and a smaller amount of ash which reached the sedimentation area. Violet patches in host rock also indicate an environment with better oxygenated sediments and probably with lower bioproductivity during the deposition of the bentonite. The lower sulphur content of this bentonite could as well reflect more suppressed microbial sulphate reduction in a marine environment with increased salinity.

An outstanding feature of both studied bentonites is P and Ca peaks (Fig. 5) in the host rock directly above the bentonites. This effect is greater after the thicker Kinnekulle Bentonite and less significant after the smaller BII Bentonite. Note that the previously discussed sulphur peak occurs in the Kinnekulle bed just below the Ca- and P-rich host rock. Increased productivity after the ash-fall, bottom oxygen deficit, enhanced sulphate reduction and raised alkalinity near the sediment–water interface could possibly favour precipitation of calcium carbonate from the dissolved Ca-hydrocarbonate. The enrichment of P, which is a fundamental limiting nutrient for marine life (Filippelli 2002; E. Kiipli et al. 2010), is more controversial. Phosphorus mostly remineralized in the course of organic matter breakdown on the seafloor and most of it externally recycled in shallow marine environments. Studies of modern volcanic ashes indicate that some ash-falls might provide a considerable extra source of P for marine environments through rapid release of the element from ash (Jones & Gislason 2008). The recorded P_2O_5 values in the Kinnekulle and BII bentonites are rather low; however, it does not exclude the possibility that some of P was released during very early stages of ash transformation. We suppose that P-enrichment above the studied bentonites could have been induced either (1) by the release of P during anoxic breakdown of organic matter under increased flux of organic matter to the seafloor or (2) by the desorption of phosphorous species or leaching of P from ash particles, and thereafter fixation in alkaline mud above the ash beds.

CONCLUSIONS

1. Both the Kinnekulle and BII bentonites in the Kuressaare section were formed from a single volcanic eruption as evidenced by the stability of the composition of phenocrysts through the entire section of the bentonite. In Norway and Sweden a multiple eruption deposit has been interpreted in the Kinnekulle Bentonite (Batchelor 2014), thus our study area received only some of the ash events. Sanidine phenocryst compositions that have been used in many previous studies for proving the correlations of volcanic ash beds are stable throughout the vertical section and therefore serve as a good discrimination criterion. Phenocrysts from the redeposited parts of bentonites can also be used for correlation. Sanidine composition can be analysed very precisely (±0.5 mol%) with advanced XRD technologies.
2. The Kinnekulle Bentonite, one of the major volcanic ash beds of the Phanerozoic, was formed from the eruption of longer duration, with a maximum power of the eruption in the middle. Pyroclastic mineral grain size distribution and immobile trace element composition point to the layered and heterogeneous nature of the primary ash bed.
3. The BII Bentonite formed from a less voluminous eruption of shorter duration. Its full thickness was accumulated from the redeposition of volcanic material in shallow-sea areas.
4. For reliable trace-element-based correlation of thick bentonites the bulk chemical composition of several samples covering the whole section should be studied. Lower parts of the bentonites originating from direct ash-falls are of correlative value. However, the mobility of trace elements should be checked in advance.
5. The Kinnekulle ash-fall and to a lesser extent the BII ash-fall had a notable effect on the chemistry of juxtaposed marine sediments. Peak concentrations of Ca and P directly above both bentonites and the increased S content near bentonite contacts show that the ash-falls triggered significant fluctuations in biotic and geochemical cycles in shallow marine settings.

Acknowledgements. We greatly appreciate constructive criticism and numerous helpful comments of the reviewer Richard A. Batchelor and an anonymous referee. This study was supported by the Estonian Ministry of Education and Research through the target research project No. SF0140016s09.

REFERENCES

Altaner, S. P., Hower, J. & Whitney, G. 1984. Model for K-bentonite formation – evidence from zoned K-bentonites in the disturbed belt, Montana. *Geology*, **12**, 412–415.

Batchelor, R. A. 2009. Geochemical "Golden Spike" for Lower Palaeozoic metabentonites. *Earth and Environmental Science Transactions of the Royal Society of Edinburgh*, **99**, 177–187.

Batchelor, R. A. 2014. Geochemistry of Upper Ordovician metabentonites and their cognate apatite microphenocrysts from Norway and Sweden. *GFF*, **136**, 387–397.

Bergström, S. M., Huff, W. D., Kolata, D. R. & Bauert, H. 1995. Nomenclature, stratigraphy, chemical fingerprinting, and areal distribution of some Middle Ordovician K-bentonites in Baltoscandia. *Geologiska Föreningens i Stockholm Förhandlingar (GFF)*, **117**, 1–13.

Bergström, S. M., Huff, W. D., Kolata, D. R., Yost, D. A. & Hart, C. 1997. A unique Middle Ordovician K-bentonite bed succession at Röstånga, S. Sweden. *GFF*, **119**, 231–244.

Brusewitz, A. M. 1988. Asymmetric zonation of a thick Ordovician K-bentonite bed at Kinnekulle, Sweden. *Clays and Clay Minerals*, **36**, 349–353.

Dahlqvist, P., Calner, M., Kallaste, T., Kiipli, T. & Siir, S. 2012. Geochemical variations within the mid-Silurian Grötlingbo Bentonite (Gotland, Sweden): discriminating between magmatic composition, ash transport fractionation and diagenetic effects. *GFF*, **134**, 273–282.

Duggen, S., Olgun, N., Croot, P., Hoffmann, L., Dietze, H., Delmelle, P. & Teschner, C. 2010. The role of airborne volcanic ash for the surface ocean biogeochemical iron-cycle. *Biogeosciences*, **7**, 827–844.

Filippelli, G. M. 2002. The global phosphorus cycle. In *Phosphates: Geochemical, Geobiological, and Materials Importance* (Kohn, M., Rakovan, J. & Hughes, J., eds), *Mineralogy & Geochemistry*, **48**, 391–425.

Fisher, R. V. & Schmincke, H. U. 1984. *Pyroclastic Rocks*. Springer-Verlag, Berlin, Heidelberg, New York, Tokyo, 472 pp.

Fortey, R. A. & Cocks, L. R. M. 2005. Late Ordovician global warming – The Boda event. *Geology*, **33**, 405–408.

Grim, R. E. & Güven, N. 1978. Bentonites, geology, mineralogy, properties and uses. *Developments in Sedimentology*, **24**, 1–256.

Hetherington, C. J., Nakrem, H. A. & Potel, S. 2011. Note on the composition and mineralogy of upper Silurian bentonites from the Ringerike District: implications for local and regional stratigraphic correlation and sedimentation. *Norwegian Journal of Geology*, **91**, 181–192.

Hints, L., Männik, P., Hints, O. & Hints, R. 2008. Discovery of the Ordovician Kinnekulle K-bentonite at the Põõsaspea cliff, NW Estonia. *Estonian Journal of Earth Sciences*, **57**, 192–196.

Hints, O., Kallaste, T. & Kiipli, T. 1997. Mineralogy and micropalaeontology of the Kinnekulle altered volcanic ash bed (Ordovician) at Pääsküla, North Estonia. *Proceedings of the Estonian Academy of Sciences, Geology*, **46**, 107–118.

Hints, O., Hints, L. & Meidla, T. 2003. Effects of the Ordovician Kinnekulle ash-fall recorded in northern Estonia. *Bulletin of the Geological Society of Denmark*, **50**, 115–123.

Hints, R., Kirsimäe, K., Somelar, P., Kallaste, T. & Kiipli, T. 2006. Chloritization of Late Ordovician K-bentonites from the northern Baltic Palaeobasin – influence from source material or diagenetic environment? *Sedimentary Geology*, **191**, 55–66.

Hints, R., Kirsimäe, K., Somelar, P., Kallaste, T. & Kiipli, T. 2008. Multiphase Silurian bentonites in the Baltic Palaeobasin. *Sedimentary Geology*, **209**, 69–79.

Huff, W. D., Kolata, D. R., Bergström, S. M. & Zhang, Y.-S. 1996. Large-magnitude Middle Ordovician volcanic ash falls in North America and Europe: dimensions, emplacement and post-emplacement characteristics. *Journal of Volcanology and Geothermal Research*, **73**, 285–301.

Huff, W. D., Bergström, S. M. & Kolata, D. R. 2010. Ordovician explosive volcanism. In *The Ordovician Earth System* (Finney, S. C. & Berry, W. B. N., eds), *The Geological Society of America Special Paper*, **466**, 13–28.

Jones, M. T. & Gislason, S. R. 2008. Rapid releases of metal salts and nutrients following the deposition of volcanic ash into aqueous environments. *Geochimica et Cosmochimica Acta*, **72**, 3661–3680.

Kaljo, D., Grytsenko, V., Kallaste, T., Kiipli, T. & Martma, T. 2014. Upper Silurian stratigraphy of Podolia revisited: carbon isotopes, bentonites and biostratigraphy. *GFF*, **136**, 136–141.

Kallaste, T. & Kiipli, T. 2006. New correlations of Telychian (Silurian) bentonites in Estonia. *Proceedings of the Estonian Academy of Sciences, Geology*, **55**, 241–251.

Kastner, M. 1971. Authigenic feldspars in carbonate rocks. *American Mineralogist*, **56**, 1403–1442.

Kiipli, E., Kallaste, T. & Kiipli, T. 2004. Metabentonites of the Pirgu Stage (Ashgill, Upper Ordovician) of the East Baltic. In *WOGOGOB-2004, 8th Meeting of the Working Group on the Ordovician Geology of Baltoscandia, May 13–18, Tallinn and Tartu, Estonia, Abstracts and Field Guidebook* (Hints, O. & Ainsaar, L., eds), pp. 53–54. Institute of Geology, University of Tartu.

Kiipli, E., Kiipli, T., Kallaste, T. & Ainsaar, L. 2010. Distribution of phosphorus in the Middle and Upper Ordovician Baltoscandian carbonate palaeobasin. *Estonian Journal of Earth Sciences*, **59**, 247–255.

Kiipli, E., Kiipli, T., Kallaste, T. & Siir, S. 2012. Al_2O_3/TiO_2 ratio of the clay fraction of Late Ordovician–Silurian carbonate rocks as an indicator of paleoclimate of the Fennoscandian Shield. *Palaeogeography, Palaeoclimatology, Palaeoecology*, **365**–**366**, 312–320.

Kiipli, T., Kallaste, T., Kiipli, E. & Orlova, K. 2006. Upper Ordovician volcanic ash beds. In *Kerguta (565) Drill Core* (Põldvere, A., ed.), *Estonian Geological Sections*, 7, 15–18.

Kiipli, T., Kiipli, E., Kallaste, T., Hints, R., Somelar, P. & Kirsimäe, K. 2007. Altered volcanic ash as an indicator of marine environment, reflecting pH and sedimentation rate – example from the Ordovician Kinnekulle bed of Baltoscandia. *Clays and Clay Minerals*, **55**, 177–188.

Kiipli, T., Jeppsson, L., Kallaste, T. & Söderlund, U. 2008a. Correlation of Silurian bentonites from Gotland and the East Baltic using sanidine phenocryst composition, and biostratigraphical consequences. *Journal of the Geological Society*, **165**, 211–220.

Kiipli, T., Orlova, K., Kiipli, E. & Kallaste, T. 2008b. Use of immobile trace elements for the correlation of Telychian bentonites on Saaremaa Island, Estonia, and mapping of volcanic ash clouds. *Estonian Journal of Earth Sciences*, **57**, 39–52.

Kiipli, T., Kallaste, T. & Nestor, V. 2010a. Composition and correlation of volcanic ash beds of Silurian age from the eastern Baltic. *Geological Magazine*, **147**, 895–909.

Kiipli, T., Kallaste, T., Nestor, V. & Loydell, D. K. 2010b. Integrated Telychian (Silurian) K-bentonite chemostratigraphy and biostratigraphy in Estonia and Latvia. *Lethaia*, **43**, 32–44.

Kiipli, T., Radzevičius, S., Kallaste, T., Kiipli, E., Siir, S., Soesoo, A. & Voolma, M. 2012. The Geniai Tuff in the southern East Baltic area – a new correlation tool near the Aeronian/Telychian stage boundary, Llandovery, Silurian. *Bulletin of Geosciences*, **87**, 695–704.

Kiipli, T., Kallaste, T., Kiipli, E. & Radzevičius, S. 2013. Correlation of Silurian bentonites based on the immobile elements in the East Baltic and Scandinavia. *GFF*, **135**, 152–161.

Kiipli, T., Kallaste, T., Nielsen, A., Schovsbo, N. & Siir, S. 2014a. Geochemical discrimination of the Upper Ordovician Kinnekulle Bentonite in the Billegrav-2 drill core section, Bornholm, Denmark. *Estonian Journal of Earth Sciences*, **63**, 264–270.

Kiipli, T., Radzevičius, S. & Kallaste, T. 2014b. Silurian bentonites in Lithuania: correlations based on sanidine phenocryst composition and graptolite biozonation – interpretation of volcanic source regions. *Estonian Journal of Earth Sciences*, **63**, 18–29.

Kiipli, T., Soesoo, A. & Kallaste, T. 2014c. Geochemical evolution of Caledonian volcanism recorded in the sedimentary rocks of the eastern Baltic region. In *New perspectives on the Caledonides of Scandinavia and Related areas* (Corfu, F., Gasser, D. & Chew, D. M., eds), *Geological Society Special Publications*, **390**, 177–192.

Kiipli, T., Dahlquist, P., Kallaste, T., Kiipli, E. & Nõlvak, J. 2015. Upper Katian (Ordovician) bentonites in the East Baltic, Scandinavia and Scotland: geochemical correlation and volcanic source interpretation. *Geological Magazine*, dx.doi.org/10.1017/S001675681400051X.

Kolata, D. R., Frost, J. K. & Huff, W. D. 1987. Chemical correlation of K-bentonite beds in the Middle Ordovician Decorah Subgroup, upper Mississippi Valley. *Geology*, **15**, 208–211.

Laufeld, S. & Jeppsson, L. 1976. Silicification and bentonites in the Silurian of Gotland. *GFF*, **98**, 31–44.

Männik, P., Põldvere, A., Nestor, V., Kallaste, T., Kiipli, T. & Martma, T. 2014. The Llandovery–Wenlock boundary interval in west-central continental Estonia: an example from the Suigu (S-3) core section. *Estonian Journal of Earth Sciences*, **63**, 1–17.

Perrier, V., Meidla, T., Tinn, O. & Ainsaar, L. 2012. Biotic response to explosive volcanism: ostracod recovery

after Ordovician ash-falls. *Palaeogeography, Palaeoclimatology, Palaeoecology*, **365–366**, 166–183.

Põlma, L. 1967. On the transitional area between the northern and axial lithofacies zones of the East Baltic Ordovician. *Proceedings of the Estonian Academy of Sciences, Chemistry, Geology*, **16**, 272–275 [in Russian].

Rampino, M. R., Self, S. & Stothers, R. B. 1988. Volcanic winters. *Annual Review of Earth and Planetary Science*, **16**, 73–99.

Ray, D. C., Collings, A. V. J., Worton, G. J. & Jones, G. 2011. Upper Wenlock bentonites from Wren's Nest Hill, Dudley: comparisons with prominent bentonites along Wenlock Edge, Shropshire, England. *Geological Magazine*, **148**, 670–681.

Somelar, P., Kirsimäe, K., Hints, R. & Kirs, J. 2010. Illitization of Early Paleozoic K-bentonites in the Baltic Basin: decoupling of burial- and fluid-driven processes. *Clays and Clay Minerals*, **58**, 388–398.

Torsvik, T. H. & Rehnström, E. F. 2003. The Tornquist Sea and Baltic Avalonia docking. *Tectonophysics*, **362**, 67–82.

Winchester, J. A. & Floyd, P. A. 1977. Geochemical discrimination of different magma series and their differentiation products using immobile elements. *Chemical Geology*, **20**, 325–343.

Kahe paksu Ordoviitsiumi bentoniidi sisemine stratifikatsioon: magmaliste, setteliste, keskkonna ja diageneetiliste tunnuste dešifreerimine

Sven Siir, Toivo Kallaste, Tarmo Kiipli ja Rutt Hints

Uuriti 26 proovi kahest suurest vulkaanilise tuha kihist, Kinnekulle ja BII Bentoniidist Kuressaare K-3 puuraugust Saaremaalt, eesmärgiga välja selgitada kihtide sisemine geokeemiline ning mineraloogiline heterogeensus. On kirjeldatud ja interpreteeritud märke materjali fraktsioneerumisest vulkaanituha transpordil ning ümbersettimisel merebasseinis ja tunnuseid elementide diageneetilisest ümberjaotumisest. Valdavaks autigeenseks mineraaliks Kinnekulle Bentoniidis on illiit-smektiit vähesema kaaliumpäevakivi lisandiga kihi äärtel. BII Bentoniit koosneb kloriit-smektiidist ja illiit-smektiidist. Magmaliste fenokristallide sanidiini ja biotiidi koostise stabiilsus mõlema kihi vertikaalläbilõikes tõendab, et mõlema bentoniidi lähtematerjal kuhjus ühest vulkaanipurskest. Sanidiini koostise stabiilsus (±0,5 mol%) mõlema bentoniidi läbilõikes kinnitab, et see on usaldusväärne kriteerium bentoniidikihtide identifitseerimiseks ja korrelatsiooniks. Mikroelementide jaotus osutab, et Zr, Ga, Rb, Nb, Ti ja Th püsisid immobiilsena vulkaanilise tuha muutumisel bentoniidiks, peegeldades hästi vulkaanilise tuha algset koostist. Siiski on märgata väikest Nb, Ti ja Y liikuvust kihtide kontaktil ümbriskivimiga. Märkimisväärsed S, Ca ja P akumulatsioonid kihtide kontaktidel ümbriskivimiga on tunnuseks, et vulkaanituha kuhjumine põhjustas märgatavaid hälbeid madalmere ning settelises keskkonnas.